

Receptance Coupling for High-Speed Machining Dynamics Prediction

Tony L. Schmitz

Department of Mechanical and Aerospace Engineering
University of Florida
Gainesville, Florida 32611, USA

Timothy J. Burns

Mathematical and Computational Sciences Division
National Institute of Standards and Technology
Gaithersburg, Maryland 20899-8910, USA

ABSTRACT

We apply receptance coupling techniques to predict the tool-point frequency response for high-speed machining applications. Building on early work of Duncan [4], Bishop and Johnson [2], and more recent work of Ewins, et al. [5],[6], we develop an analytic expression for the frequency response at the free end of the milling cutter from: 1) an analytic model of the tool; 2) an experimental measurement of the holder/spindle sub-assembly; and 3) a set of empirical connection parameters. These parameters are extracted from a single measurement of the tool/holder/spindle assembly at a known tool overhang length using nonlinear least squares estimation. The assembly model can then be used to predict changes in the tool-point receptance for setup variations, such as tool length. The resulting tool-point frequency response is used to calculate the associated stability lobe diagram, which defines regions of stable and unstable cutting zones as a function of chip width and spindle speed and is used to select appropriate machining parameters. A description of the receptance coupling method, as well as a discussion of the system model and selected connection parameters, are provided. Extensive experimental results are also presented.

1. Introduction

The implementation of high-speed machining for the manufacture of discrete parts, especially in the aerospace industry, has led to the replacement of complicated assemblies of fastened sheet-metal pieces by stronger, lighter, monolithic aluminum parts, at a considerable cost savings [10]. Here, following Smith and Tlusty [9], we mean by high-speed machining a cutting operation that takes place at a tooth-engagement frequency that is close to the vibration frequency (or a substantial integer fraction thereof) of the most flexible mode of the machine/tool system. To use high-speed machining to manufacture monolithic parts with deep pockets out of aluminum, long, slender, fluted cutting tools are required, causing a lack of stiffness that can lead to unwanted self-excited vibrations in the system, known as regenerative tool chatter.

For such processes, an accurate frequency response function is required for the prediction of the deflection of the assembly at the tool point and, subsequently, chatter

avoidance [1],[3]. Referring to Figure 1, suppose the tool point is subjected to harmonic vertical forcing with frequency ω and amplitude F . The response of the structure is assumed to be linear elastic. Hence, its vertical deflection due to the forcing will also have frequency ω . If the amplitude of the deflection at the tool point is X , so that the steady-state harmonic motion at the tip is given by $X \exp i\omega t$, then what is required is the *direct receptance* $G(\omega)=X/F$, over the frequency interval of interest. Using the negative real part of this receptance function, optimal cutting parameters can be determined that will maximize the chatter-free material removal rate (see for example, Tlusty, et al. [11], Davies, et al. [3]). For example, the stability lobe diagram giving the limiting stable depth of cut as a function of frequency is determined by the formula

$$b_{critical} = \frac{-1}{K_s \mu \min\{\text{Re}[G(\omega)]\}z},$$

where K_s and μ are constants, and z is the number of flutes on the tool.

A direct experimental approach to this problem is simply to excite the tool point for each tool/holder/spindle assembly using, for example, an instrumented hammer, and then record the frequency response of the combined system over the range of interest. This can be time-consuming, and many manufacturers lack the equipment and qualified personnel to obtain the necessary information.

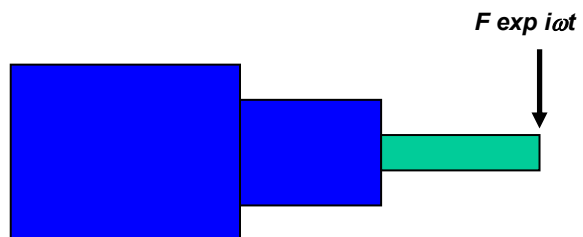


Figure 1. Spindle/holder/tool assembly. Frequency response function is needed to predict deflection at tool point.

In the work we present here, we continue the development of a new alternative approach to the determination of the tool-point response, using receptance coupling substructure analysis (RCSA) [2],[4],[5],[6]. Our method combines limited experimental displacement frequency response measurements of the holder/spindle substructure, which need to be performed only once, with closed-form analytical expressions for the deflection and slope frequency response functions of the tool, modeled as a free-free beam using elementary beam theory (see Duncan [4], Bishop and Johnson [2]). A long-term goal of this approach is to create a database of the required tool-point frequency response information for each commercial holder/spindle assembly.

The basic outline of the paper is as follows. In Section 2, we present our combined analytical-experimental method, together with some essential approximations, for receptance coupling applied to a spindle/holder/tool system. In Section 3, we present a justification for the approximations we make. Section 4 contains an application of our method. We demonstrate its usefulness in a typical example involving tool tuning, where we consider the tool-point dynamics of a system with a Tribos tool holder and six long-overhang endmills, each with the same diameter, but with successively increasing length-to-diameter ratios. In the final section, we present some concluding remarks.

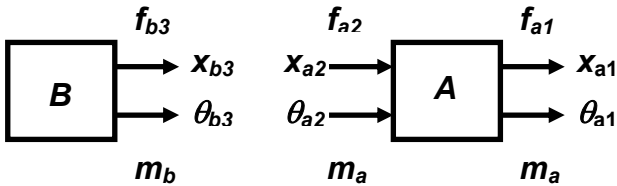


Figure 2. Schematic of the two substructures, spindle/holder (B) and tool (A).

2. Tool-Point Receptance

Our combined analytical/experimental approach to the prediction of the deflection/force frequency response of the combined structure at the tool point is as follows. Referring to Figure 2, the basic idea, following Duncan [4] and Bishop and Johnson [2], is to consider the entire spindle/holder/tool structure to be an assembly of two linear elastic substructures, that are linked at their ends by two coordinates. In the present application, the tool is essentially a free-free beam in flexure (see Figure 3).

To model the tool, we use the analytic, closed-form expressions for the tip receptances of a uniform Euler-Bernoulli beam that are tabulated in the text of Bishop and Johnson [2, Table 7.1(c)]. These receptances give the deflections and slopes at each tip of the free-free beam in response to harmonic virtual forces and moments applied at the tips. For $m = 1..2, n = 1..2$, where m is the coordinate and n is the location of force application, let

$$A_{mn} = \begin{bmatrix} H_{mn}(\omega) & L_{mn}(\omega) \\ N_{mn}(\omega) & P_{mn}(\omega) \end{bmatrix}$$

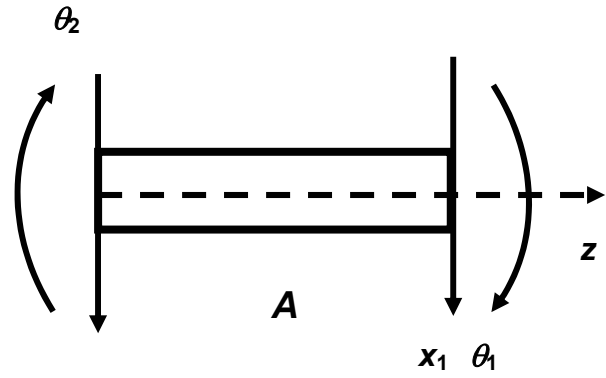


Figure 3. Schematic of tool modeled as a free-free beam, showing positive tip forces and moments.

It is straightforward to translate from the Bishop and Johnson notation to our notation; for example,

$$H_{11} = \alpha_{11}, \quad P_{11} = \alpha_{11}', \quad L_{21} = \alpha_{01}' = N_{12} = \alpha_{11}''.$$

The coordinate responses to virtual forces and moments are then given as follows.

$$\begin{pmatrix} x_{a1} \\ \theta_{a1} \end{pmatrix} = A_{11} \begin{pmatrix} f_{a1} \\ m_{a1} \end{pmatrix} + A_{12} \begin{pmatrix} f_{a2} \\ m_{a2} \end{pmatrix}, \quad (1)$$

$$\begin{pmatrix} x_{a2} \\ \theta_{a2} \end{pmatrix} = A_{21} \begin{pmatrix} f_{a1} \\ m_{a1} \end{pmatrix} + A_{22} \begin{pmatrix} f_{a2} \\ m_{a2} \end{pmatrix}.$$

On the other hand, to determine the frequency response of the spindle/holder assembly, we rely on experimental measurements. For the moment, assume that we can determine the entire spindle/holder B frequency response experimentally. Like a beam (see Figure 4), at the connection with the tool, there are two coordinates, x_3 (θ_3) corresponding to vertical deflection (slope).

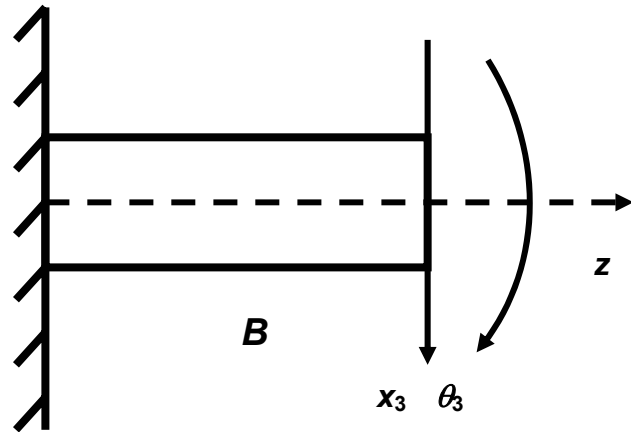


Figure 4. Schematic of spindle/holder, indicating tip coordinates where joint is made with tool.

If the system is excited at its tip with frequency ω by a force $f_{b3} \exp i\omega t$ (moment $m_{b3} \exp i\omega t$), then by the assumption of linear elasticity, the system exhibits a linear, harmonic response with the same frequency,

$$\begin{pmatrix} x_3 \\ \theta_3 \end{pmatrix} = \begin{pmatrix} x_{b3} \\ \theta_{b3} \end{pmatrix} \exp i\omega t.$$

Dropping the time-dependent exponential terms, we thus have that the deflection (slope) of the spindle/holder structure in response to a force (moment) are given by the linear relationship

$$\begin{pmatrix} x_{b3} \\ \theta_{b3} \end{pmatrix} = \mathbf{B}_{33} \begin{pmatrix} f_{b3} \\ m_{b3} \end{pmatrix}, \quad \mathbf{B}_{33}(\omega) = \begin{bmatrix} H_{33}(\omega) L_{33}(\omega) \\ N_{33}(\omega) P_{33}(\omega) \end{bmatrix}. \quad (2)$$

Referring to Figure 5, what we want to determine is the direct deflection receptance $\mathbf{G}_{11}(\omega) = \mathbf{X}_1 / \mathbf{F}_1$ for the combined spindle/holder/tool structure \mathbf{C} .

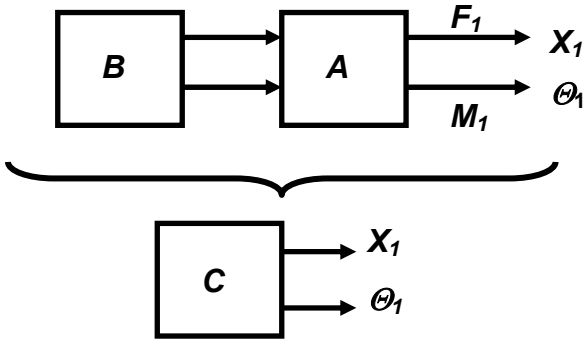


Figure 5. Schematic of combined spindle/holder/tool structure.

Using the same kind of reasoning as before, when subjected to harmonic disturbances, the combined structure \mathbf{C} will respond elastically with the same frequency,

$$\begin{pmatrix} X_1 \\ \theta_1 \end{pmatrix} = \mathbf{C}_{11} \begin{pmatrix} F_1 \\ M_1 \end{pmatrix}, \quad \mathbf{C}_{11}(\omega) = \begin{bmatrix} \mathbf{G}_{11}(\omega) \Lambda_{11}(\omega) \\ \Sigma_{11}(\omega) \Pi_{11}(\omega) \end{bmatrix}. \quad (3)$$

It is the first entry in the first column of the receptance matrix \mathbf{C}_{11} that is required for a tool chatter stability analysis.

There are two fundamental difficulties with making the assumption of two independent substructures and then simply using classical receptance coupling to predict the frequency response of the tool-point deflection. First, the only measurement we can make with confidence at the tool insertion location 3 is the direct receptance $H_{33}(\omega)$. This means that the other receptances $P_{33}(\omega)$, $L_{33}(\omega)$, and $N_{33}(\omega)$ are unavailable. In the following section, we present an argument that it is a good approximation in the coupled system to set $P_{33} = N_{33} = L_{33} = 0$.

The second fundamental difficulty with our method is that we cannot assume that subsystems \mathbf{A} and \mathbf{B} are directly linked at the two sets of coordinates at locations 2 and 3 in Figure

2. That is, we cannot simply join the two substructures at locations 2 and 3 by assuming that $x_{b3} = x_{a2}$, $\theta_{b3} = \theta_{a2}$ in Figure 2, and that the forces and moments balance at these junctions, because there are complicated contact conditions in the overlap region where the holder fastens the tool. Following some of our previous work on the development of the method presented here [8], we make the assumption that the connection between the tool and holder can be modeled adequately by coupling the deflection (slope) of the two subsystems together using a viscously damped linear (torsional) spring. Thus, we assume the virtual force $f_{b2} \exp i\omega t$ (moment $m_{b2} \exp i\omega t$) is applied through the springs, so that

$$\begin{aligned} k_x(x_{b3} - x_{a2}) + c_x(\dot{x}_{b3} - \dot{x}_{a2}) &= f_{a2}, & f_{a2} + f_{b3} &= 0, \\ k_\theta(\theta_{b3} - \theta_{a2}) + c_\theta(\dot{\theta}_{b3} - \dot{\theta}_{a2}) &= m_{a2}, & m_{a2} + m_{b3} &= 0. \end{aligned} \quad (4)$$

The spring (damping) parameters k_x, k_θ (c_x, c_θ) must still be determined. Our method for estimating the values of the connection coefficients will be discussed below.

Once again assuming harmonic excitation of the structure at a fixed frequency, the connection constraints (4) can be written in terms of a "complex coupling" matrix as follows.

$$\begin{aligned} \mathbf{K} \begin{pmatrix} x_{b3} - x_{a2} \\ \theta_{b3} - \theta_{a2} \end{pmatrix} &= \begin{pmatrix} f_{a2} \\ m_{a2} \end{pmatrix} = - \begin{pmatrix} f_{b3} \\ m_{b3} \end{pmatrix}, \\ \mathbf{K}(\omega) &= \begin{bmatrix} K_x(\omega) & 0 \\ 0 & K_\theta(\omega) \end{bmatrix}, \\ \begin{pmatrix} K_x \\ K_\theta \end{pmatrix} &= \begin{pmatrix} k_x + i\omega c_x \\ k_\theta + i\omega c_\theta \end{pmatrix}. \end{aligned} \quad (5)$$

Setting

$$\begin{pmatrix} X_1 \\ \theta_1 \end{pmatrix} = \begin{pmatrix} x_{a1} \\ \theta_{a1} \end{pmatrix}, \quad \begin{pmatrix} F_1 \\ M_1 \end{pmatrix} = \begin{pmatrix} f_{a1} \\ m_{a1} \end{pmatrix}, \quad (6)$$

we solve for \mathbf{G}_{11} in several steps.

By (5),

$$\begin{pmatrix} x_{b3} - x_{a2} \\ \theta_{b3} - \theta_{a2} \end{pmatrix} = \mathbf{K}^{-1} \begin{pmatrix} f_{a2} \\ m_{a2} \end{pmatrix}, \quad (7)$$

and by (2) and (4),

$$\begin{pmatrix} x_{b3} \\ \theta_{b3} \end{pmatrix} = \mathbf{B}_{33} \begin{pmatrix} f_{b3} \\ m_{b3} \end{pmatrix} = -\mathbf{B}_{33} \begin{pmatrix} f_{a2} \\ m_{a2} \end{pmatrix}. \quad (8)$$

Using (1), (6), (7) and (8), we get

$$\begin{aligned} \begin{pmatrix} x_{b3} - x_{a2} \\ \theta_{b3} - \theta_{a2} \end{pmatrix} &= -\mathbf{B}_{33} \begin{pmatrix} f_{a2} \\ m_{a2} \end{pmatrix} - \mathbf{A}_{21} \begin{pmatrix} F_1 \\ M_1 \end{pmatrix} - \mathbf{A}_{22} \begin{pmatrix} f_{a2} \\ m_{a2} \end{pmatrix} \\ &= \mathbf{K}^{-1} \begin{pmatrix} f_{a2} \\ m_{a2} \end{pmatrix}. \end{aligned}$$

Hence,

$$\mathbf{T} \begin{pmatrix} f_{a2} \\ m_{a2} \end{pmatrix} = -\mathbf{A}_{21} \begin{pmatrix} F_1 \\ M_1 \end{pmatrix}, \quad \mathbf{T} = \mathbf{K}^{-1} + \mathbf{A}_{22} + \mathbf{B}_{33}. \quad (9)$$

To proceed further, we require that the matrix \mathbf{T} be invertible. This is equivalent to the following condition on the determinant of \mathbf{T} ,

$$\det \mathbf{T} \neq 0. \quad (10)$$

By (1) and (6),

$$\begin{pmatrix} X_1 \\ \theta_1 \end{pmatrix} = \mathbf{A}_{11} \begin{pmatrix} F_1 \\ M_1 \end{pmatrix} + \mathbf{A}_{12} \begin{pmatrix} f_{a2} \\ m_{a2} \end{pmatrix},$$

so using (3) and (9), and assuming (10), we get the desired receptance matrix for the spindle/holder/tool modeled as two subsystems linked by linear viscous springs,

$$\mathbf{C}_{11} = \mathbf{A}_{11} - \mathbf{A}_{12} \mathbf{T}^{-1} \mathbf{A}_{21}. \quad (11)$$

It is now straightforward to determine the desired tool point receptance $\mathbf{G}_{11}(\omega)$. To simplify the notation, let

$$\begin{aligned} \mathbf{H} &= \mathbf{H}_{33} + \mathbf{H}_{22}, \quad \mathbf{L} = \mathbf{L}_{33} + \mathbf{L}_{22}, \\ \mathbf{N} &= \mathbf{N}_{33} + \mathbf{N}_{22}, \quad \mathbf{P} = \mathbf{P}_{33} + \mathbf{P}_{22}. \end{aligned} \quad (12)$$

We get that

$$\begin{aligned} \mathbf{G}_{11} = \frac{X_1}{F_1} &= \mathbf{H}_{11} - \frac{\mathbf{H}_{12}}{\det \mathbf{T}} \left[\mathbf{H}_{21} \left(\mathbf{P} + \frac{1}{K_\theta} \right) - \mathbf{N}_{21} \mathbf{L} \right] \\ &\quad - \frac{\mathbf{L}_{12}}{\det \mathbf{T}} \left[-\mathbf{H}_{21} \mathbf{N} + \mathbf{N}_{21} \left(\mathbf{H} + \frac{1}{K_x} \right) \right]. \end{aligned} \quad (13)$$

3. Frequency Equation of the Composite System

We note that the determinant of the matrix $\mathbf{T}(\omega)$ appears twice in the denominator of the expression for $\mathbf{G}_{11}(\omega)$. Thus the requirement (10) that this determinant be nonzero over the frequency range of interest is important. Because of this, in this section, we examine the matrix \mathbf{T} more closely. In addition, we derive some approximations for use in applications of the tool-point receptance formula (13) in the next section.

By (9), $\mathbf{T} = \mathbf{K}^{-1} + \mathbf{A}_{22} + \mathbf{B}_{33}$. The first observation we make about \mathbf{T} is that it is the sum of properties of three "substructures" that make up the spindle/holder/tool assembly. The latter two terms comprise properties of the tool and the spindle/holder system, respectively, while the first term is the inverse of the complex coupling matrix \mathbf{K} , defined in (5). The nonzero entries of \mathbf{K} determine the stiffness and viscous damping properties that join the tool to

the holder. We could have chosen to treat the springs and dashpots as a third substructure, but we have used a simpler coupling approach instead, as described by Ewins [5] and Ewins and Ferreira [6]. It is easy to see that, over a finite interval of frequencies, if we hold the viscous damping coefficients constant but increase the stiffness of the two springs, then in the limit as the stiffnesses go to infinity, $\mathbf{K}^{-1} = \mathbf{0}$. In this case, receptance coupling reduces to connecting the two structures by rigid joints at the two adjacent sets of deflection and slope coordinates, as depicted in Figure 5.

A second observation about \mathbf{T} is the following. Because matrix addition is associative, we can imagine that the viscous springs are first attached to the tool; that is, we may assume that $\mathbf{T} = \bar{\mathbf{A}}_{22} + \mathbf{B}_{33}$, where

$$\bar{\mathbf{A}}_{22} = \mathbf{K}^{-1} + \mathbf{A}_{22}. \quad (14)$$

Now,

$$\det \bar{\mathbf{A}}_{22} = \frac{1}{K_x K_\theta} + \frac{P_{22}}{K_x} + \frac{H_{22}}{K_\theta} + \det \mathbf{A}_{22}. \quad (15)$$

By (15), it follows that, as

$$k_x, k_\theta \rightarrow \infty \quad (c_x, c_\theta \text{ fixed}), \quad \det \bar{\mathbf{A}}_{22} = \det \mathbf{A}_{22}.$$

So far, we have not assumed that there is any dissipation in the free-free beam model of the tool. This means that the receptance matrix $\mathbf{A}_{22}(\omega)$ is real, and the values of ω at which all of its entries simultaneously become infinite correspond to the resonant frequencies of the free-free beam. Furthermore, the values of ω that satisfy the equation

$$\det \mathbf{A}_{22}(\omega) = 0 \quad (16)$$

determine the cantilever frequencies of beam \mathbf{A} . Thus, if we set the viscous damping coefficients equal to zero, $c_x = 0, c_\theta = 0$, the beam changes from free-free to clamped-free as the stiffnesses of the connecting springs become infinitely large. In the more realistic case in which $c_x > 0, c_\theta > 0$, we can write

$$\begin{pmatrix} K_x \\ K_\theta \end{pmatrix} = \begin{pmatrix} k_x \left[1 + i\omega \frac{c_x}{k_x} \right] \\ k_\theta \left[1 + i\omega \frac{c_\theta}{k_\theta} \right] \end{pmatrix}.$$

Once again, for large spring constants relative to the damping coefficients, we see that, over a finite frequency range, $K_x \approx k_x, K_\theta \approx k_\theta$, so in this case we expect the frequencies of the beam to be close to those of the undamped clamped-free beam.

Now, we use these two observations about \mathbf{T} to draw some useful conclusions. If we expand the determinant of \mathbf{T} using the notation in (12), we get that

$$\det \mathbf{T} = \frac{1}{K_x K_\theta} + \frac{P}{K_x} + \frac{H}{K_\theta} + HP - LN. \quad (17)$$

Expanding the last two terms in (17), we find that

$$HP - LN = \det \mathbf{A}_{22} + \det \mathbf{B}_{33} + H_{22}P_{33} + H_{33}P_{22} - L_{22}N_{33} - L_{33}N_{22}.$$

Hence, we can rewrite (17) as follows,

$$\det \mathbf{T} = \det \bar{\mathbf{A}}_{22} + \det \mathbf{B}_{33} + \frac{P_{33}}{K_x} + \frac{H_{33}}{K_\theta} + H_{22}P_{33} + H_{33}P_{22} - L_{22}N_{33} - L_{33}N_{22}. \quad (18)$$

By reciprocity, $L_{22} = N_{22}$, and for the free-free beam model of the tool, we can show that, over the frequency interval of interest,

$$abs P_{22}(\omega) \gg \max[abs(H_{22}(\omega)), abs(L_{22}(\omega))]. \quad (19)$$

To proceed further, we make the following assumption: *the tool (substructure A) is much more flexible than the spindle/holder (substructure B)*. Mathematically, this assumption can be written in terms of the complex moduli,

$$\begin{aligned} abs H_{33} &\ll abs H_{22}, & abs L_{33} &\ll abs L_{22}, \\ abs N_{33} &\ll abs N_{22}, & abs P_{33} &\ll abs P_{22}. \end{aligned} \quad (20)$$

By (18), we have that

$$\det \mathbf{T} = \det \bar{\mathbf{A}}_{22} + \det \mathbf{B}_{33} + \left(\frac{1}{K_x} + H_{22} \right) P_{33} + \left(\frac{1}{K_\theta} + P_{22} \right) H_{33} - 2L_{22}L_{33}. \quad (21)$$

Dividing (21) through by P_{22} , we have, by (19) and (20), for the last four terms that

$$\begin{aligned} \frac{\det \mathbf{B}_{33}}{P_{22}} + \left(\frac{1}{K_x} + H_{22} \right) \frac{P_{33}}{P_{22}} + \left(\frac{1}{K_\theta P_{22}} + 1 \right) H_{33} - 2L_{33} \frac{L_{22}}{P_{22}} \\ \approx \left(\frac{1}{K_\theta P_{22}} + 1 \right) H_{33}. \end{aligned}$$

Therefore, we have that

$$\det \mathbf{T} \approx \det \bar{\mathbf{A}}_{22} + \left(\frac{1}{K_\theta} + P_{22} \right) H_{33}. \quad (22)$$

Thus we may make the approximation that

$$P_{33} = N_{33} = L_{33} = 0, \quad (23)$$

because these terms do not appear in (22). In the next section, we use (23) in the formula for $\mathbf{G}_{11}(\omega)$ given by (15) to estimate the tool-point response for a specific spindle/holder/tool system.

4. Method for Determining Coupling Parameters and an Application

In this section, we assume (23) and apply the approximate expression (15) for the tool tip receptance derived in the preceding section to the problem of *tool tuning* [11],[3],[8]. The basic idea of this method is to change the tool point dynamics, in order to avoid chatter at a given maximal machining center rpm, for example, by adjusting the parameters that define the tool; in the present case, tool length is the single adjustable parameter. As will be demonstrated, both the frequency and amplitude of the tool-point receptance vary significantly with the tool length. We include comparisons between predicted and experimentally measured results for a given spindle with a Tribos tool holder and six tools with length/diameter ratios that vary from 6:1 to 11:1. We also demonstrate that the receptance modeling approach can be used in the present application to predict the tool tip deflection given only the connection parameters for the shortest and longest tools in the six tool set, thus reducing by two thirds the amount of work required for the complete range of tool lengths. Additional examples of the application of receptance coupling to tool tuning may be found in the paper by Schmitz, et al. [8].

The measured frequency response of the spindle/holder system is shown in Figure 6, which gives plots of the real and imaginary parts of the direct deflection tip receptance $H_{33}(\omega)$ as functions of the frequency.

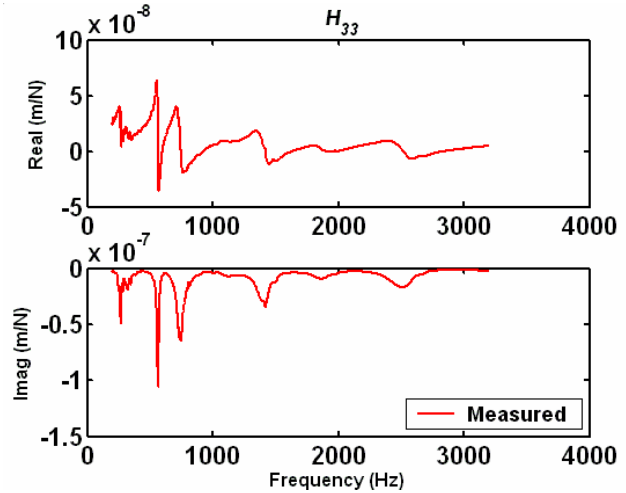


Figure 6. Measured frequency response of tip of spindle/holder system.

As discussed by Bishop and Johnson [2], it is straightforward to add uniform hysteretic damping ζ to the free-free beam model of the tool. This can be done by changing the elastic modulus for carbide, $E = 585.3$ GPa, to the complex modulus $E(1+i\zeta)$, and then using the same closed-form analytic free-free beam tip receptance expressions. For the work we present here, however, we have found that it is

adequate to make the assumption that $\zeta=0$. In each case, the carbide tool diameter is $D=12$ mm, and the six overhang lengths vary from 72 mm to 132 mm, so that the length-to-diameter ratios vary in whole numbers from 6:1 to 11:1. Because the tools are fluted, we have calculated that they have an effective diameter of $D=11.8$ mm; this is the value used for D to compute the cross-sectional second moment of inertia I for the six tools tested.

The four spring (damping) connection parameters $k_x, k_\theta (c_x, c_\theta)$ must still be determined for each tool. Our current approach to estimating these constants for a given system is as follows. First, for each tool length we utilize the nonlinear least-squares software *lsqnonlin* in the Matlab Optimization Toolbox [7] to determine real parameter fits that minimize the residual to within 10^{-12} ; call these six sets of parameter values the *best fits*. Comparisons between the experimentally measured spindle/holder/tool direct deflection tip receptance and that obtained using Equation (15) derived above are given for the shortest and longest tools in Figures 7 and 8, respectively; comparisons for the remaining four tools are similar. In addition to observing that our four-parameter model based on RCSA gives reasonable approximations for the measured frequency response behaviors, we note the increased flexibility and lower-frequency resonance of the longest, most flexible tool, and also the contribution of the spindle/holder mode near 1500 Hz to the response of the shortest (6:1) overhang tool.

To demonstrate the predictive value of our modeling approach, we use logarithmic interpolation of the best-fit parameters for the longest and shortest tools (Figure 9) to predict the direct tool-point deflection receptances of the remaining four tools; see Figure 10. We note that, for all six tools, the dominant frequency decreases with increasing tool length. However, in the case of the 9:1 overhang tool, there is an interesting “dynamic absorber” effect arising from the interaction between the spindle/holder system dynamics and the tool dynamics. This decreased flexibility response could be usefully exploited to maximize the material removal rate in some industrial high-speed machining applications requiring longer-overhang tools.

5. Concluding Remarks

We have presented a receptance coupling method for predicting the tool-point frequency response of a long-overhang high-speed machining structure consisting of a spindle, holder, and tool. Even though the method entails a number of approximations, the predictions made by the resulting model in a tool tuning application, using only two sets of experimental measurements for the composite system together with a single measurement of the deflection response of the spindle/holder subsystem, show that our approach provides useful predictions of the dynamic tool-point response of the combined system.

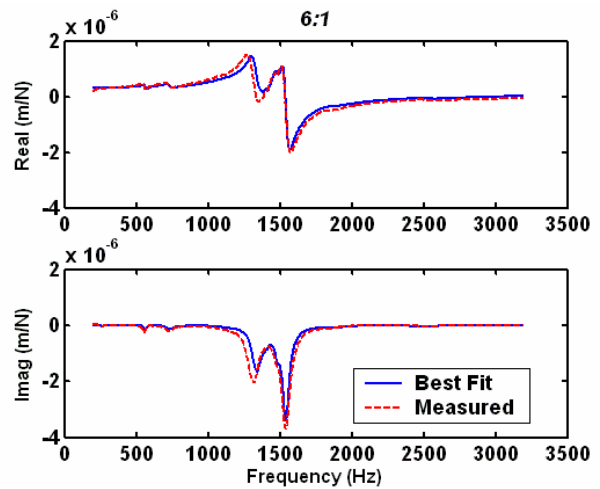


Figure 7. Comparison between measured frequency response and predicted response using Equation (15) for shortest overhang tool with best-fit connection parameters.

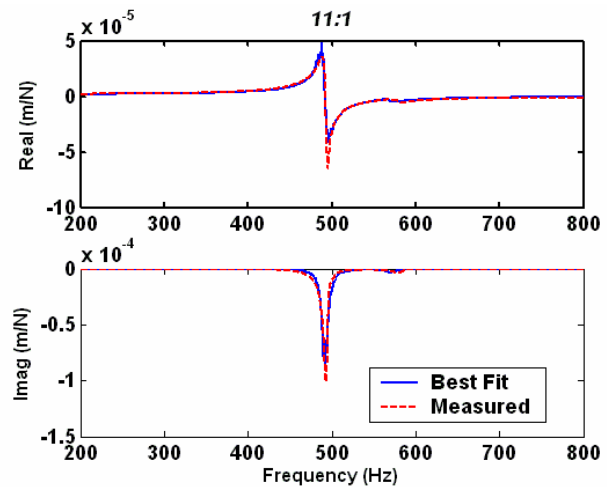


Figure 8. Comparison between measured frequency response and predicted response using Equation (15) for longest overhang tool with best-fit connection parameters.

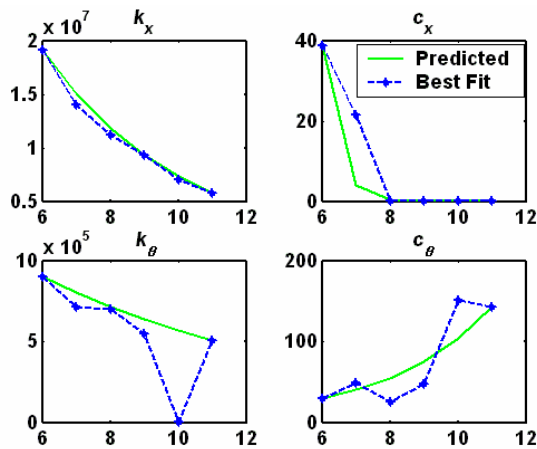


Figure 9. Comparison between best-fit connection parameter values and logarithmic interpolation of best-fit values for shortest and longest tools.

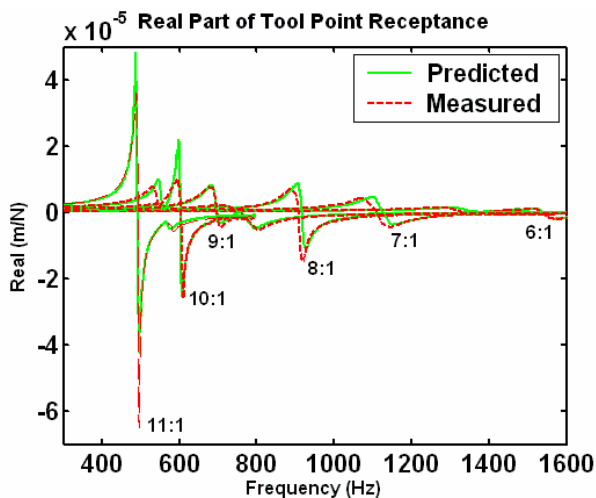


Figure 10. Real parts of measured and predicted tool-point receptances $G_{11}(\omega)$ for tools with six different length-to-diameter ratios.

Acknowledgments

We would like to acknowledge helpful interactions with Matt Davies and Mike Kennedy.

Certain commercial products are identified in this paper in order to document computational and laboratory experiments adequately. Identification of such products does not constitute endorsement by NIST, nor does it imply that these are the most suitable products for the task. U.S. Government work in the public domain of the United States.

References

- [1] Altintas, Y., and Budak, E., Analytical Prediction of Stability Lobes in Milling, *CIRP Annals*, **44**(1): 357-362 (1995).
- [2] Bishop, R.E.D. and Johnson, D.C., *The Mechanics of Vibration*, Cambridge University Press, Cambridge, U.K, 1960.
- [3] Davies, M.A., Dutterer, B., Pratt, J., and Schaut, A., On the Dynamics of High-Speed Machining with Long, Slender Endmills, *CIRP Annals*, **41**(2): 55-60 (1998).
- [4] Duncan, W.J., *Mechanical Admittances and their Applications to Oscillation Problems*, Ministry of Supply, Aeronautical Research Council Reports and Memoranda No. 2000, London: His Majesty's Stationery Office, 1947.
- [5] Ewins, D.J., *Analysis of Modified or Coupled Structures Using FRF Properties*, Imperial College London, Dynamics Section, Mechanical Engineering, Report No. 86002, 1986.
- [6] Ferreira, J., and Ewins, D., Nonlinear Receptance Coupling Approach Based on Describing Functions, Proceedings of the 14th International Modal Analysis Conference, Dearborn, Michigan, pp. 1034-1040, 1995.
- [7] MathWorks, *Matlab 6.5.0 Release 13: High-Performance Numeric Computation and Visualization Software*, Natick, Massachusetts, 2002.
- [8] Schmitz, T.L., Davies, M.A., and Kennedy, M.D., Tool Point Frequency Response Prediction for High-Speed Machining by RCSA, *Journal of Manufacturing Science and Technology*, Transactions of the ASME, **123**: 700-707 (2001).
- [9] Smith, S., and Tlusty, J., An Overview of Modeling and Simulation of the Milling Process, *Journal of Engineering for Industry*, Transactions of the ASME, **113**: 169-175 (1991).
- [10] Smith, S., Winfough, W., and Halley, J., The Effect of Tool Length on Stable Metal Removal Rate in High-Speed Milling, *CIRP Annals*, **47**(1): 307-310 (1998).
- [11] Tlusty, J., Zaton, W., and Ismail, F., Stability Lobes in Milling, *CIRP Annals*, **32**(1): 309-313 (1983).